

# Influence of Traumatic Brain Injury on Extracellular Tau Elimination at the Blood-Brain Barrier

Maxwell Eisenbaum (✉ [meisenbaum@roskampinstitute.org](mailto:meisenbaum@roskampinstitute.org))

Roskamp Institute <https://orcid.org/0000-0002-1967-9450>

Andrew Pearson

Roskamp Institute

Arissa Gratkowski

Roskamp Institute

Benoit Mouzon

Roskamp Institute

Michael Mullan

Roskamp Institute

Fiona Crawford

Roskamp Institute

Joseph Ojo

Roskamp Institute

Corbin Bachmeier

Roskamp Institute

---

## Research

**Keywords:** Mural cells, tau, pericytes, endothelial cells, traumatic brain injury, blood-brain barrier, caveolin-1, angiopoietin-1, angiopoietin-2, mfsd2a

**Posted Date:** May 17th, 2021

**DOI:** <https://doi.org/10.21203/rs.3.rs-522678/v1>

**License:**  This work is licensed under a Creative Commons Attribution 4.0 International License.

[Read Full License](#)

---

# Abstract

Repetitive head trauma has been associated with the accumulation of tau species in the brain. Our prior work showed brain vascular mural cells contribute to tau processing in the brain, and that these cells progressively degenerate following repetitive mild traumatic brain injury (r-mTBI). The current studies investigated the role of the cerebrovasculature in the elimination of extracellular tau from the brain, and the influence of r-mTBI on these processes. Following intracranial injection, the levels of exogenous tau residing in the brain were elevated in a mouse model of r-mTBI at 12 months post-injury compared to r-sham mice, indicating reduced tau elimination from the brain following head trauma. This may be the result of decreased caveolin-1 mediated tau efflux at the blood-brain barrier (BBB), as the caveolin inhibitor, methyl- $\beta$ -cyclodextrin, significantly reduced tau uptake in isolated cerebrovessels and significantly decreased the basolateral-to-apical transit of tau across an *in vitro* model of the BBB. Moreover, we found that the upstream regulator of endothelial caveolin-1, Mfsd2a, was elevated in r-mTBI cerebrovessels compared to r-sham, which coincided with a decreased expression of cerebrovascular caveolin-1 at 6 months post-injury. Lastly, angiopoietin-1, a mural cell-derived protein governing endothelial Mfsd2a expression, was secreted to a greater extent from r-mTBI cerebrovessels compared to r-sham animals. Thus, in the chronic phase post-injury, release of angiopoietin-1 from degenerating mural cells downregulates caveolin-1 expression in brain endothelia, resulting in decreased tau elimination across the BBB, which may describe the accumulation of tau species in the brain following head trauma.

## Introduction

Exposure to repetitive head injuries sustained in the military or contact sports has been associated with an increased risk for the development of chronic neurodegenerative diseases, including chronic traumatic encephalopathy (CTE) (McKee et al., 2009). Though the underlying mechanism behind the progression of CTE is unclear, the neuropathologic presentation has become apparent through postmortem examination. CTE appears to be a primary tauopathy characterized, in part, by a perivascular accumulation of pathological hyperphosphorylated tau at the depth of cortical sulci (McKee et al., 2016). Tau, which primarily supports the functions of microtubules in neurons, has traditionally been viewed as an intracellular protein, but recent research has revealed an important pathological role of extracellular tau in neurodegenerative progression (Medina and Avila, 2014). Furthermore, traumatic brain injury (TBI) results in elevated levels of extracellular tau in the interstitial fluid (ISF) of the central nervous system (CNS) (Marklund et al., 2009), which has been correlated with adverse clinical outcomes (Öst et al., 2006; Magnoni et al., 2012).

Though extracellular tau has an important role in disease pathogenesis, the mechanisms by which extracellular tau is eliminated from the brain and the influence of TBI on these processes has been largely unexplored. While extracellular solutes can be eliminated from the brain through bulk flow or perivascular pathways, a major route of elimination occurs via transit across the blood-brain barrier (BBB). Microdialysis studies investigating tau movement in brain interstitial fluids have suggested that tau may be more dynamically linked to the blood than to cerebrospinal fluid (Yamada et al., 2011; Wang et al.,

2018), implicating possible interactions with the BBB. Several pathogenic proteins have been shown to cross the BBB (Deane et al., 2009; Sui et al., 2014; Banks, 2015), including tau (Banks et al., 2016), but the processes driving the BBB transit of tau are not fully understood, particularly following trauma to the brain. Tau elimination mechanisms may share a common route, as it has been suggested that degradation and perivascular clearance may be responsible for a greater magnitude of extracellular tau elimination than bulk flow to the CSF (Yamada et al., 2011).

Our recent work found brain vascular mural cells progressively degenerate at chronic time points following repetitive mild traumatic brain injury (r-mTBI) in a mouse model of concussion (Ojo et al., 2021). Moreover, these effects were associated with reduced cerebrovascular tau uptake in freshly isolated cerebrovessels from r-mTBI animals. Notably, the decrease in tau uptake post-injury coincided with significant reductions in cerebrovascular caveolin-1 levels in the mouse r-mTBI model. Caveolin-1 is an integral membrane component for the formation and function of caveolae-mediated cerebrovascular transcytosis. Additionally, similar decreases in caveolin-1 were observed in cerebrovessels from human TBI brain specimens when compared to non-injured control brains (Ojo et al., 2021). While few studies have investigated the relationship between tau and cerebrovascular caveolin-1, it has been reported that mice with decreased caveolin-1 expression exhibit elevated levels of total and phosphorylated tau in the brain (Head et al., 2010; Bonds et al., 2019). Caveolin-1 activity in brain endothelial cells is primarily regulated by the lysolipid transporter Mfsd2a (major facilitator superfamily domain-containing protein-2a) (Ben-Zvi et al., 2014; Andreone et al., 2017). Mfsd2a plays a critical role in maintaining BBB permeability, and it was found that overexpression of Mfsd2a after brain injury is neuroprotective (Zhao et al., 2020). While it has been observed that Mfsd2a levels downregulate in the acute phase following brain injury (Eser Ocak, Ocak, Sherchan, Gamdzyk, *et al.*, 2020), the state of cerebrovascular Mfsd2a at more chronic stages post-injury and the effect on caveolin-1 levels and tau elimination across the BBB have not been investigated. The goal of this study is to investigate the mechanisms influencing tau elimination at the BBB and determine the chronic effects of head trauma on these processes.

## Materials And Methods

### Materials

Primary human brain vascular pericytes (HBVP) (cat#1200), primary human brain microvascular endothelial cells (HBMEC) (cat#1000), and associated culture reagents were purchased from Sciencell Research Laboratories (Carlsbad, CA, USA). Fibronectin solution (cat#F1141), poly-L-lysine solution (cat#P4707), methyl- $\beta$ -cyclodextrin (cat#C4555), heparin (cat#H3393-10KU) and Hanks' balanced salt solution (HBSS)(cat#H8264) were purchased from MilliporeSigma (St. Louis, MO, USA). Lucifer yellow dextran (10 kDa) and the human tau enzyme linked immunosorbent assay (ELISA) (cat#KHB0041) were purchased from Invitrogen Corp. (Carlsbad, CA, USA). Mammalian protein extraction reagent (M-PER) (cat#78505), Halt enzyme inhibitor cocktails (cat#78442), and the bicinchoninic acid (BCA) protein assay (cat#23225) were purchased from ThermoFisher Scientific (Waltham, MA, USA). The ELISA kit for mouse Major facilitator superfamily domain containing 2 (Mfsd2a) was purchased from LifeSpan BioSciences,

Inc. (Seattle, WA, USA) (cat#LS-F17827-1). The ELISA kit for mouse caveolin-1 (caveolin-1) was purchased from MyBioSource, Inc. (San Diego, CA, USA) (cat#MBS721447). The ELISA kit for mouse angiopoietin-1 (Ang-1) (cat#NBP2-62857) was purchased from Novus Biologicals (Littleton, CO, USA). The ELISA kit for mouse angiopoietin-2 (Ang-2) (cat#MANG20) was purchased from R&D Systems (Minneapolis, MN, USA). Recombinant human tau-441 was purchased from rPeptide (Watkinsville GA, USA) (cat#T-1001-2). Recombinant biotinylated human tau-441 (cat#T08-54BN) and DYRK1A-phosphorylated and biotinylated human tau-441 (cat#T08-50RNB) were purchased from SignalChem (Richmond, BC, Canada).

## Animals

Both male and female mice [Human tau (hTau) (cat# 005491) and wild-type (C57BL/6) (cat# 000664)] were purchased from the Jackson Laboratory (Bar Harbor, ME, USA). The hTau mice express six isoforms of human tau on a C57BL/6 background, but do not express murine tau, as previously described (Andorfer et al., 2003). The hTau genotype was confirmed after purchase using PCR from a tail snip via a third party (Transnetyx, Cordova, TN, USA). The hTau mice were generated to examine tau pathology at various timepoints following head trauma for separate set of studies. The tissue derived from this cohort was used in the present studies to examine cerebrovascular protein changes over time following brain injury. All studies used mice housed 3 per cage under standard laboratory conditions ( $23 \pm 1^\circ\text{C}$ ,  $50 \pm 5\%$  humidity, and a 12-hour light/dark cycle) with free access to food and water throughout the study. All experiments using animals were performed under protocols approved by the Institutional Animal Care and Use Committee (IACUC) of the Roskamp Institute.

## Brain injury protocol

Repetitive mild traumatic brain injury (r-mTBI) was administered using a mouse model of closed head injury as previously characterized by our group (Mouzon et al., 2012, 2014). Briefly, after being 1.5 L/min of oxygen and 3% isoflurane, mice had their head shaved and were secured in a mouse stereotaxic apparatus (Stoelting) mounted with an electromagnetic controlled impact device (Leica) and a heating pad to maintain their body temperature. Before impact, a 5mm blunt metal impactor tip was retracted and positioned midway in relation to the sagittal suture. The injury was triggered using the myNeuroLab controller (Leica) at a strike velocity of 5m/s, strike depth of 1.0mm, and a dwell time of 200 milliseconds. Randomly assigned three-month-old mice received 2 injuries per week, approximately 72 hours apart, for 3 months (r-mTBI). As a control, sham animals did not receive the brain injury, but were exposed to anesthesia for the same length of time as the injured mice and under the same paradigm (2 exposures per week for 3 months). Mice were euthanatized at 24 hours, 3 months, 6 months after the final brain injury or anesthesia exposure. The sample sizes for the r-sham and r-mTBI groups were the same for each post-injury time point: 24 hours ( $n = 4$ ), 3 months ( $n = 4$ ), and 6 months ( $n = 5$ ). For the intracranial tau injection studies, the sample sizes for the r-sham and r-mTBI groups were  $n = 5$  and  $n = 4$ , respectively, for each tau species. Of note, two mice from the intracranial injection studies died prior to completion of the 2-hour post-injection endpoint, following intracranial tau administration.

## Isolation of brain fractions

The cerebrovasculature was isolated from mouse tissue as characterized and described by our group previously (Bachmeier et al., 2014). Briefly, fresh mouse cortices were ground in 5 ml of ice-cold HBSS with 6–8 passes of a Teflon pestle in a glass Dounce homogenizer. A 250  $\mu$ l aliquot of homogenate was collected with lysis buffer (M-PER) supplemented with phenylmethanesulfonyl fluoride (1mM) and Halt protease and phosphatase inhibitor cocktail. An equal volume of 40% dextran solution was added to the remaining brain homogenate for a final concentration of 20% dextran and immediately centrifuged at 6000g for 15 min at 4°C. This procedure results in a pellet at the bottom of the container (cerebrovasculature) and a compact mass at the top of the solution (parenchyma) separated by a clear dextran interface (soluble fraction, i.e., non-cell associated). The freshly isolated vessels were collected and immediately used for the *ex vivo* studies described below.

## Tau Aggregation

Enriched fractions of low molecular weight aggregated tau were generated as previously described (Mirbaha et al., 2017). Briefly, biotin-labeled tau (4.35  $\mu$ M) was incubated with freshly prepared Heparin (1  $\mu$ M) for 6 hours at 37°C. Aggregation was confirmed using Thioflavin T. The solution was passed through a 100 kDa MWCO filter (Corning) and centrifuged at 14,000 x g for 25 min at 4°C. The concentrated, aggregate enriched fraction was collected and stored at -80°C. The filtered fraction of seed competent monomers was then concentrated using a 30 kDa MWCO filter (Corning) and centrifuged at 14,000 x g for 25 min at 4°C. The protein concentration was determined using a btau ELISA. Misfolding of the seed competent monomeric fraction was confirmed using dot blot. A 1  $\mu$ l, concentration matched (50 ng/ml) aliquot of untreated monomeric btau, seed competent btau and aggregate enriched btau (50 ng/ml) was placed on a nitrocellulose membrane for 30 minutes at room temperature before blocking in 10% BSA in tris buffered saline with 0.1% Tween-20 (TBS-T) overnight at 4°C. The membrane was incubated for 1 hour in MC1 (MC1, 1:1000 diluted in TBS-T with 5% BSA). The membrane was vigorously washed with TBS-T, then incubated in horseradish peroxidase-conjugated anti-mouse secondary antibody (goat anti-mouse IgG 1:1000 in TBS-T with 5% BSA) for 1 hour at room temperature. After an additional wash in TBS-T, SuperSignal West Femto Maximum Sensitive Substrate (ThermoFisher) was used for chemiluminescence detection and signal intensity ratios were quantified with the ChemiDoc TM XRS (Bio-Rad). MC1 is a conformation-dependent tau antibody generously provided by Dr. Peter Davies, The Feinstein Institute for Medical Research, Bronx, NY, USA.

## Tau elimination

For the temporal tau elimination studies, 6 wild-type mice (9 months of age) were anesthetized via inhalation using a 3% isoflurane / oxygen mix and maintained at 37°C using a homeothermic blanket. mice were stereotaxically injected into the brain with (50  $\mu$ g/ml) human biotinylated recombinant tau (441) in 3 $\mu$ l of PBS (0.5 mm anterior to the bregma, 2 mm lateral to the midline, and 3 mm below the surface of the skull) as per our prior methods (Paris et al., 2011). In a separate cohort of mice, 10 kDa lucifer yellow dextran (LyD) (100 mg/ml) was stereotaxically injected into the brain in the same manner as above, to provide context for the tau studies, as LyD does not readily cross the BBB (Natarajan, Northrop and Yamamoto, 2017). Mice were euthanized at 10 minutes, 30 minutes, 1 hour, 2 hours, 4

hours, 8 hours, and 24 hours after the intracranial injection. The brain was harvested, and each hemisphere was homogenized with probe sonication in 500  $\mu$ l of lysis buffer. The half-life for both  $\tau$  and LyD was determined using nonlinear regression and a one phase decay fit (GraphPad Prism 8.0, GraphPad Software, Inc). The value at time = 0 (y-intercept) was used as the theoretical initial concentration in the brain and the values at each time point were calculated as a percentage of this initial concentration.

## **Tau residence in the brain**

Biotinylated tau species and LyD were stereotaxically injected into r-sham and r-mTBI wild-type mice (12 months post-injury), in the same manner as the temporal studies above, and euthanized 2 hours after the intracranial injection. The brain homogenate was evaluated for biotin-labeled tau using a modified hTau ELISA (Invitrogen). The ELISA was performed according to the manufacturer's protocol, using stock biotin labeled tau as the standard and excluding the 1-hour incubation step with a biotin-conjugated primary antibody. Furthermore, each stereotaxic injection included 10 kDa lucifer yellow dextran (LyD) (80 mg/ml) to account for any nonspecific leakage out of the brain, as LyD typically demonstrates low BBB permeability (Natarajan, Northrop and Yamamoto, 2017). LyD fluorescence was analyzed using a microplate spectrofluorometer (Cytation 3). With respect to tau, all samples were evaluated for tau remaining in the brain and normalized to LyD for each time point. To assess LyD alone, the amount of LyD at each time point was normalized to total protein content as determined using the BCA assay.

## **Caveolin-1 and Mfsd2a expression in r-mTBI mice**

Cerebrovessels from r-mTBI and r-sham mice at 24 hours, 3 months and 6 months post-injury were collected using lysis buffer (M-PER) supplemented with phenylmethanesulfonyl fluoride (1mM) and Halt protease and phosphatase inhibitor cocktail. The cell lysates were analyzed for caveolin-1 and Mfsd2a by ELISA and normalized to total protein content using the BCA protein assay.

### **Tau uptake and caveolin inhibition ex vivo**

Freshly isolated cerebrovessels from wild-type mice (9 months of age) were pre-treated with methyl- $\beta$ -cyclodextrin (0, 1, and 10 mM) for 30 minutes at 37°C followed by treatment with 5 ng/ml  $\tau$  for 1 hour at 37°C. Following the treatment period, the extracellular media was removed, and the cerebrovessels were washed with ice-cold HBSS. Cell lysates were collected using lysis buffer (M-PER) supplemented with phenylmethanesulfonyl fluoride (1 mM) and Halt protease and phosphatase inhibitor cocktail. The cell lysates were analyzed for total tau by ELISA and normalized to total protein content using the BCA protein assay.

### **Angiopoietin 1 modulates HBMEC expression of Mfsd2a in vitro**

Fully confluent HBMECs were treated with 2.5 ng/ml of Ang-1 or a vehicle in ECM for 24 hours. Cells were washed with HBSS and cell lysates were collected using lysis buffer as described previously. The cell lysates were analyzed for Mfsd2a by ELISA and normalized to total protein content using the BCA assay.

## Cerebrovascular angiopoietin 1/2 secretion ex vivo

Freshly isolated cerebrovessels from r-mTBI and r-sham mice 6 months post-injury were incubated in ECM for 72 hours at 37°C. Following the incubation, the extracellular media was collected, the cerebrovessels were washed in ice-cold HBSS, then collected in lysis buffer as described previously. The extracellular media was evaluated for secretion of angiopoietin-1 and angiopoietin-2 by ELISA and normalized to the corresponding cell lysate total protein content using the BCA protein assay.

## BBB assay co-culture

Using HBVP and HBMEC cells, a contact coculture version of our previously characterized in vitro BBB model (Bachmeier 2010) was used to evaluate tau transcytosis. Briefly, HBVP were seeded at 25,000 cells / cm<sup>2</sup> onto the exterior portion of poly-L-lysine coated 24-well 0.4 μm-pore membrane inserts. One hour after HBVP seeding, HBMEC were seeded at 50,000 cells / cm<sup>2</sup> onto the interior membrane of the fibronectin-coated insert to establish a polarized monolayer. The layer of cells separates this system into an apical (“blood” side) and basolateral (“brain” side) compartment. The basolateral compartment was exposed to monomeric or aggregated biotinylated tau (200 ng/ml) in the presence or absence of MβCD (10 mM), while fresh media was placed in the apical compartment. The inserts containing media were exposed to the wells containing biotinylated tau and incubated at 37°C. The basolateral compartment was sampled at time 0 to establish the initial concentration of biotinylated tau. Samples were collected from the apical compartment at 0, 30, and 60 min to assess the rate of bttau transcytosis across the cell monolayer (basolateral-to-apical) and analyzed for bttau using a modified hTau ELISA. Furthermore, each basolateral compartment was exposed to a known paracellular marker, 10 kDa lucifer yellow dextran (LyD 10 μM), to monitor cellular integrity and/or nonspecific permeability, as we previously described (Bachmeier, Mullan and Paris, 2010). The apparent permeability (Papp) was determined using the equation  $P_{app} = 1 / AC_0 * (dQ / dt)$ , where A represents the surface area of the membrane, C<sub>0</sub> is the initial concentration of bttau in the basolateral compartment, and dQ / dt is the amount of bttau appearing in the apical compartment in the given time period.

## Statistical analysis

Randomization and blinding procedures were employed. Quantitative data were plotted as mean ± standard deviation. Statistical analysis was performed using GraphPad Prism 8.0 (GraphPad Software, Inc RRID:SCR\_002798). The Shapiro-Wilk test was completed to assess normality. Tau uptake was evaluated for significance by ANOVA and the Bonferroni post hoc test with multiple comparisons. Tau elimination, as well as cav-1 and mfsd2a expression were evaluated for significance as determined by two-way ANOVA Bonferroni post hoc test with multiple comparisons. For comparisons between two groups including tau transcytosis, angiopoietin secretion and stimulation studies, statistical significance was analyzed using a two-tailed unpaired Student’s t-test or a Mann-Whitney U test. For all analyses, a p value of ≤ 0.05 was considered statistically significant.

## Results

# Tau residence time

We evaluated the elimination profile of tau from the brain following intracranial injection and determined the half-life of exogenous bttau residing in the brain to be 41 minutes (Fig. 1). In contrast, the half-life of 10 kDa LyD, which does not readily cross the BBB, was nearly 3-times greater at 114 minutes (Fig. 1A). We further evaluated the influence of r-mTBI on the elimination of exogenous tau species from the brain, collecting the brain 2 hours after the intracranial bttau injection. A two-way ANOVA evaluating the effect of r-mTBI and tau species on tau residence time did not demonstrate a statistically significant interaction effect [ $F_{(3,28)} = 2.235, p = 0.106$ ]. A significant main effect was observed with respect to injury [ $F_{(1,28)} = 9.359, p = 0.005$ ], and with respect to tau species [ $F_{(3,20)} = 9.359, p < 0.001$ ]. Post hoc Bonferroni tests with multiple comparisons between r-mTBI and r-sham revealed a significant increase ( $p = 0.003$ ) in monomeric tau residence in r-mTBI ( $2.56 \pm 1.40$ ) compared to r-sham ( $1.08 \pm 0.53$ ). While the other bttau species (i.e. phosphorylated, seed competent, and aggregate enriched) showed an increased bttau residence time in the brain post-injury compared to each respective r-sham group, including a nearly 2-fold elevation of the aggregate enriched bttau species, the values for each of these bttau species did not reach statistical significance (Fig. 1B). Furthermore, additional post hoc Bonferroni tests with multiple comparisons evaluated each of the bttau species under r-mTBI conditions. The amount of exogenous phosphorylated bttau residing in the brain ( $1.49 \pm 0.51$ ) was not significantly different compared to the amount of monomeric bttau ( $2.56 \pm 1.40$ ) (Fig. 1). However, the amount of exogenous seed competent ( $0.67 \pm 0.12$ ) and aggregate enriched ( $0.94 \pm 0.51$ ) bttau in the brain under r-mTBI conditions were significantly lower than the amount of monomeric bttau in the brain, 3.8-fold ( $p < 0.001$ ) and 2.7-fold ( $p = 0.003$ ) respectively (Fig. 1B). Of note, no statistically significant differences in the amount of dextran residing in the brain were observed between the r-mTBI and r-sham groups for any of the bttau species, indicating the effects of r-mTBI on tau elimination from the brain were not due to alterations in BBB integrity (data not shown).

## Tau uptake and caveolin-1 inhibition ex vivo

Freshly isolated cerebrovessels were treated with previously established doses of a known modulator of caveolin-1, methyl- $\beta$ -cyclodextrin (Jozic et al., 2019; Potje et al., 2019) before exposure to monomeric tau. A one-way ANOVA revealed a statistically significant treatment effect [ $F_{(2,12)} = 78.21, p < 0.001, n = 5$ ] on cerebrovascular tau uptake (Fig. 2A). Post hoc Bonferroni tests with multiple comparisons revealed a significant decrease ( $p < 0.001$ ) in tau uptake for both 1 mM M $\beta$ CD ( $227.8 \pm 59.83$ ) and 10 mM M $\beta$ CD ( $68.31 \pm 43.23$ ) when compared to untreated cerebrovascular tau uptake ( $549.8 \pm 78.05$ ).

## Tau transcytosis across an in vitro BBB model

In comparing the basolateral-to-apical BBB transit of each bttau species, there were no differences in the apparent permeability of each bttau species across the BBB model under control conditions. Pre-treatment with M $\beta$ CD resulted in a significant decrease (unpaired  $t$ -Test,  $t(4) = 4.830, p = 0.009, n = 3$ ) in the BBB transcytosis of monomeric tau ( $4.75 \pm 0.81$ ) compared to untreated monomeric tau transcytosis ( $28.10 \pm$

8.34) (Fig. 2B). Similarly, pre-treatment with M $\beta$ CD resulted in a significant decrease (unpaired *t*-Test,  $t(4) = 3.028$ ,  $p = 0.039$ ,  $n = 3$ ) in aggregate enriched tau transcytosis ( $7.30 \pm 1.48$ ) compared to untreated aggregate enriched tau transcytosis ( $40.97 \pm 19.20$ ) (Fig. 2B). Notably, the individual btau species did not appear to impact BBB integrity as dextran permeability across the BBB model was not different between the btau species. Likewise, treatment with M $\beta$ CD had no effect on dextran BBB permeability compared to control conditions.

## Cerebrovascular expression of caveolin-1 and mfsd2a in r-mTBI animals

A two-way ANOVA was conducted that examined the effects of r-mTBI and time on cerebrovascular caveolin-1 expression which revealed a statistically significant interaction [ $F_{(2,20)} = 18.60$ ,  $p < 0.001$ ] on caveolin-1 expression. A significant main effect was observed with respect to time [ $F_{(2,20)} = 22.39$ ,  $p < 0.001$ ], but there was no significant main effect with respect to injury [ $F_{(1,20)} = 1.243$ ,  $p = 0.278$ ]. The influence of age on caveolin-1 and Mfsd2a expression has been demonstrated recently (Yang et al., 2020), so post hoc Bonferroni tests with multiple comparisons between r-mTBI and r-sham were conducted to evaluate whether r-mTBI could influence the expression levels of cerebrovascular caveolin-1 with respect to the expression levels of r-sham at each time point. Post hoc Bonferroni tests with multiple comparisons at each time point revealed that at 24 hours post injury, there was a significant increase ( $p < 0.001$ ) in cerebrovascular caveolin-1 in r-mTBI animals ( $2055 \pm 457.7$ ) compared to sham animals ( $905.7 \pm 298.3$ ) (Fig. 3A). Alternatively, at 3 months post-injury, r-mTBI cerebrovessels ( $397.3 \pm 315.7$ ) showed a 2-fold reduction in caveolin-1 relative to r-sham animals ( $855.9 \pm 332.1$ ), while a 40% reduction in caveolin-1 was evident at 6 months post injury in r-mTBI cerebrovessels ( $504.7 \pm 148.2$ ) compared to r-sham ( $806.8 \pm 175.9$ ) though these effects did not reach statistical significance ( $p = 0.119$  and  $p = 0.362$ , respectively) (Fig. 3A). With respect to Mfsd2a, a two-way ANOVA evaluating the influence of r-mTBI and time post injury on Mfsd2a expression revealed a significant interaction [ $F_{(2,20)} = 15.09$ ,  $p < 0.001$ ] and a significant main effect with respect to time [ $F_{(2,20)} = 14.14$ ,  $p < 0.001$ ], but no significant main effect with respect to injury [ $F_{(1,20)} = 1.805$ ,  $p = 0.194$ ]. Post hoc Bonferroni tests with multiple comparisons between r-mTBI and sham revealed that at 24 hours post injury, there was a significant decrease ( $p = 0.012$ ) in cerebrovascular Mfsd2a in r-mTBI animals ( $2055.0 \pm 457.7$ ) compared to sham animals ( $905.7 \pm 298.3$ ) (Fig. 3B) and at 6 months post injury there was a significant increase ( $p < 0.001$ ) in cerebrovascular Mfsd2a in r-mTBI animals ( $540.5 \pm 82.72$ ) compared to r-sham ( $324.7 \pm 73.92$ ). At 3 months post injury, there was no significant difference ( $p = 0.515$ ) between r-mTBI ( $281.8 \pm 53.24$ ) and r-sham ( $206.9 \pm 14.34$ ).

### Ang-1/Ang-2 secretion from r-mTBI cerebrovessels ex vivo

Administration of Ang-1 to HBMECs *in vitro* over 24 hours lead to a significant increase in levels of Mfsd2a compared to untreated cells (unpaired *t*-Test,  $t(6) = 3.247$ ,  $p = 0.0175$ ,  $n = 4$ ) (Fig. 4A). At 6 months post injury, a Mann-Whitney test indicated that secreted Ang-1 levels from r-mTBI cerebrovessels ( $Mdn = 2080$ ) were significantly higher than r-sham ( $Mdn = 1206$ ) over 72 hours ( $U = 2$ ,  $p = 0.032$ ,  $n = 5$ ) (Fig. 4B).

There was no significant difference in Ang-2 secretion between r-mTBI (*Mdn* = 1337) and r-sham (*Mdn* = 1731) (Fig. 4B) ( $U = 11, p = 0.841, n = 5$ ).

## Discussion

Interest in the potential importance of extracellular tau was ignited a decade ago, when it was demonstrated that extracellular tau aggregates can induce intracellular tau misfolding (Frost, Jacks and Diamond, 2009), templated seeding, and subsequent propagation of misfolded tau from the seeded site (Clavaguera et al., 2009). As pathological tau propagation has been observed in the chronic stages of TBI and other neurodegenerative diseases, we explored potential mechanisms responsible for the elimination of extracellular tau from the brain and the influence of head trauma on these processes. Our recent work demonstrated an interaction between extracellular tau and brain vascular mural cells (pericytes and smooth muscle cells) and showed a progressive decrease in cerebrovascular tau uptake up to 12 months post-injury in our mouse r-mTBI model (Ojo et al., 2021). The reduced cerebrovascular tau uptake following r-mTBI coincided with a significant decrease in caveolin-1 levels in r-mTBI cerebrovessels compared to r-sham animals at 12 months post-injury (Ojo et al., 2021). The present studies continued this line of investigation to determine the mechanisms driving cerebrovascular tau elimination and the potential impact of head trauma on these processes.

To understand the influence of head trauma on tau elimination from the brain more broadly, we examined tau residence in the brain following intracranial injection of exogenous tau in r-mTBI animals. In other words, we determined the amount of exogenous tau residing in the brain at a given time point following intracranial administration. First, to identify an appropriate time frame in which to evaluate tau residence in the brain, we determined the temporal elimination profile of exogenous tau in the brain. The clearance of extracellular tau from the ISF has not been extensively characterized, though it appears that extracellular tau can readily enter the plasma as increases in ISF tau due to neuronal injury are reflected in the plasma shortly after injury (Yanamandra et al., 2017). After injection into the ISF, tau relocates the perivascular space within and around arteriole walls within minutes, and though it is not cleared as efficiently as A $\beta$ , recent evidence suggests they share common routes of cerebrovascular elimination (Nimmo et al., 2020). It was determined that the half-life of tau injected into the cisterna magna was less than 2 hours and the exogenous tau was detectable in the plasma within minutes of the injection (Yanamandra et al., 2017). In line with these studies, our work found the half-life of exogenous tau was approximately 41 minutes in the brain following intracranial injection. For context, we also injected a 10kDa dextran marker (LyD), that is not readily eliminated from the brain and does not cross the BBB (Natarajan, Northrop and Yamamoto, 2017), and found the half-life of LyD in the brain was 4-times the value we observed for exogenous tau (164 minutes vs. 41 minutes). Prior reporting has indicated a significantly longer half-life for tau in the brain, 11 days in mice (Yamada et al., 2015) and 20 days in humans (Sato et al., 2018). However, it is important to note these values encompassed the entire life cycle of tau, from neuronal synthesis and cellular secretion to elimination, whereas the half-life value for tau in the present study only reflects elimination from the brain. Thus, based on the elimination profile of

tau from the brain in our studies, we used a 2-hour post-injection time-point to examine the influence of head trauma on tau residence in the brain.

For each of the tau species tested, the amount of exogenous tau residing in the brain was greater in the r-mTBI animals compared to r-sham (though only the monomeric tau group reached statistical significance), indicating tau elimination from the brain was reduced following head trauma. Interestingly, the monomeric tau residing in the brain (r-sham and r-mTBI) was greater than that observed for the higher order tau species (seed competent and aggregate enriched). While studies evaluating the interactions of various tau species with brain endothelia are lacking, earlier work suggested tau aggregates, but not monomeric tau, efficiently bind to neurons and are internalized using bulk endocytosis (Wu et al., 2013). A more recent report found that both monomeric and aggregated tau can be internalized with similar efficiency in neurons, but may do so through distinct pathways (Evans et al., 2018). Solute internalization and trafficking at the BBB are both regulated by ligand binding avidity and particle size (Tian et al., 2020), which differ between tau aggregates and monomers, and may describe any differences in endothelial internalizing and trafficking amongst various tau species. Clearly further work is necessary to understand the regulatory mechanisms governing cerebrovascular tau elimination and the potential influence of head trauma on these processes.

There are several pathways through which tau can be eliminated from the brain including, but not limited to, 1) degradation, 2) perivascular drainage, and 3) BBB transcytosis. While tau has been shown to be degraded in the brain, these processes generally occur over a longer period of time (> 12 hours)(David et al., 2002; Dolan and Johnson, 2010) than the 2–3 hour elimination time-frame in our paradigm, so degradation does not appear to be a primary driver of extracellular tau elimination from the brain in our particular studies. Previous work found that paravascular tau clearance was reduced by approximately 60% following TBI and was associated with phospho-tau pathology and neurodegeneration (Iliff et al., 2014). The authors noted that if there were a tau efflux mechanism, at the BBB for example, their theory of convective bulk flow may contribute to tau ISF clearance by effectively distributing tau along the vascular bed for more efficient transcytosis (Iliff et al., 2014). That said, there has been little investigation into the transit of tau across the BBB. Banks and colleagues found that full-length tau and various truncated tau proteins readily crossed the BBB bidirectionally and entered the blood following injection into the brain (Banks et al., 2016), consistent with our intracranial tau injection studies. In line with these BBB findings, our studies employed a recently described indirect co-culture BBB model(Kurmann et al., 2021) consisting of brain endothelia and pericytes, and found the BBB transit of each tau species was greater than that observed for LyD (basolateral-to-apical). In comparing the tau species, the aggregate enriched tau showed increased BBB transcytosis compared to monomeric tau, potentially explaining the enhanced elimination of these species in the tau residence studies above. As indicated earlier, our prior work showed a correlation between tau uptake and caveolin-1 expression in isolated cerebrovessels, suggesting tau endocytosis in these cells may be mediated by caveolin-1. In the present studies, modulating caveolin-1 endocytosis with M $\beta$ CD resulted in a significant decrease in cerebrovascular tau uptake and dramatically reduced the BBB transit of both tau monomers and aggregate enriched species of tau. Along these lines, it was previously reported that mice with reduced caveolin-1 brain expression

showed elevated levels of total and phosphorylated tau in the hippocampus compared to wild-type animals (Head et al., 2010; Bonds et al., 2019). Collectively these findings indicate tau proteins can be eliminated across the BBB, which may be mediated through caveolin-1.

There is a dearth of research into the long-term effects of TBI on caveolin-1, particularly in the context of repetitive injury, but our previous studies found a significant downregulation in cerebrovascular caveolin-1 levels at 12 months post-injury in a mouse r-mTBI model (Ojo et al., 2021). Looking more acutely, our current results demonstrate an upregulation of caveolin-1 expression at 24 hours post-injury, consistent with prior reporting of increased caveolin-1 expression within the neurovascular unit during the same 24 hour period following TBI in juvenile rats (Badaut et al., 2015). However, in the rodent TBI model, the increased expression appeared to be transient, as caveolin-1 levels returned to baseline 3 days after the brain injury (Badaut et al., 2015). The acute upregulation of caveolin-1 post-injury could explain the transient increase in plasma tau levels observed immediately following sports-related concussive injury (Gill et al., 2017). In the more chronic phase post-injury, we observed decreased expression of caveolin-1 following r-mTBI at 3 and 6 months post-injury compared to r-sham, though these changes did not reach statistical significance, as they did at 12 months post-injury (Ojo et al., 2021). It has been proposed that the upregulation of caveolin-1 acutely following cerebral insult is meant to facilitate vascular repair by promoting angiogenesis and stabilizing tight junction and efflux proteins (e.g., claudin-5 and P-glycoprotein) (Badaut et al., 2015). However, as observed in the present studies, the chronic downregulation of caveolin-1 after r-mTBI could hamper elimination from the brain, leading to the accumulation of extracellular solutes such as tau, as demonstrated in other animal models where caveolin-1 is chronically diminished in the brain (Head et al., 2010; Bonds et al., 2019).

A primary regulator of caveolae-mediated transcytosis in brain endothelia is the lipid transporter Mfsd2a, which inhibits caveolae vesicle formation by modulating the lipid composition of brain endothelial membranes to suppress transcytosis (Andreone et al., 2017) and regulate BBB integrity (Yang et al., 2017). As a result, transcytosis via caveolin-1 is inversely related to Mfsd2a expression in the BBB. Correspondingly, we found cerebrovascular Mfsd2a levels were decreased at 24 hours following r-mTBI, while caveolin-1 levels were significantly increased compared to r-sham animals during this time frame. Along these lines, prior reporting showed Mfsd2a levels were significantly decreased in the acute stage after surgical brain injury (Eser Ocak, Ocak, Sherchan, Gamdzyk, *et al.*, 2020) and, interestingly, Mfsd2a upregulation was found to reverse BBB disruption by altering caveolae-based transport, providing neuroprotection following injury-induced sub-arachnoid hemorrhage (Zhao et al., 2020). In terms of the chronic phase post-injury, there is a lack of evidence regarding the response of cerebrovascular Mfsd2a to head trauma. That said, while Mfsd2a levels are generally decreased in acute conditions such as intracerebral hemorrhage, Mfsd2a has been shown to be largely upregulated in more chronic disorders such as chronic liver injury and inflammatory bowel disease (Eser Ocak, Ocak, Sherchan, Zhang, *et al.*, 2020). In line with these studies, we observed a progressive increase in cerebrovascular Mfsd2a levels in the chronic phase post-injury (6 months following r-mTBI). Certainly, more work is necessary to understand the consequence of altered Mfsd2a expression in the brain following head trauma, especially in the more chronic stages post-injury.

Mfsd2a expression in endothelial cells has been shown to be directly regulated by cerebrovascular mural cells (Ben-Zvi et al., 2014). Dysfunctional endothelial transcytosis after injury appears to be primarily driven by altered pericyte crosstalk with endothelial cells (Sun et al., 2021). To this point, the mechanism by which mural cells regulate endothelial expression of Mfsd2a and caveolin-1 is unclear, though evidence suggests the signaling factors angiopoietin-1 (Ang-1) and angiopoietin-2 (Ang-2) may play a role. Ang-1 is predominantly expressed and constitutively released by vascular mural cells (Sundberg et al., 2002; Gaengel et al., 2009). Ang-1 binds and phosphorylates the Tie2 receptor on endothelial cells to facilitate vessel assembly and stability and is a critical survival factor in preventing endothelial cell death (Kim et al., 2000). The binding of Ang-1 to endothelial Tie2 positively regulates the nuclear translocation of  $\beta$ -catenin by phosphorylation of GSK3 $\beta$  by Akt, (Zhang et al., 2011; Engelhardt and Liebner, 2014; Sweeney, Ayyadurai and Zlokovic, 2016) as a part of the  $\beta$ -catenin/mfsd2a/caveolin-1 axis that was recently demonstrated to be a key pathway governing endothelium transcytosis and integrity at the blood-retinal barrier (Wang et al., 2020). In addition, Ang-1 is known to activate the signaling pathway that downregulates plasmalemma vesicle-associated protein expression, which is also responsible for caveolin formation (Laksitorini et al., 2019). Alternatively, Ang-2 is almost exclusively secreted by endothelial cells and functions as a negative regulator of the ang-1/tie2 pathway in order to modulate vessel maturation (Hansen et al., 2010; Felcht et al., 2012). The impact of Ang-1 on caveolin-1 expression was demonstrated recently in rats, where increased caveolin-1 levels following acute brain trauma were reversed with Ang-1 treatment (Nag et al., 2017). Similarly, our studies found that treatment with Ang-1 significantly increased Mfsd2a expression in human brain endothelial cells. As such, alterations in the secretion of Ang-1 (from brain vascular mural cells) or Ang-2 (from brain endothelia) following brain injury could influence endothelial transcytosis by modulating the Mfsd2a/caveolin-1 pathway.

Previous reports have shown vascular mural cells upregulate Ang-1 in response to insults such as hypoxic conditions, while Ang-2 levels were largely decreased or unchanged (Dore-Duffy et al., 2007; Park et al., 2016). With respect to TBI, prior studies have reported a progressive decrease in Ang-1 levels in the brain (Sabirzhanov et al., 2018) and capillaries (Dore-Duffy et al., 2007) over the first 48 hours following brain injury. At later stages of brain injury, pericytes become reactive and secrete angiogenic growth factors including Ang-1 to mediate endothelial cell activity and vascular integrity (Salehi, Zhang and Obenaus, 2017). There has been a lack of work examining Ang-2 levels following TBI, however Ang-2 levels were found to be increased acutely in the brain following subarachnoid hemorrhage (Gu et al., 2016) and cold-injury (Nourhaghighi et al., 2003), but the chronic status of Ang-2 in the brain following cerebral insult is currently unknown. That said, as the time increases post-injury (days and weeks following head trauma), several studies have reported an increase in Ang-1 levels in the brain (Brickler et al., 2018; Sabirzhanov et al., 2018) and serum (Gong et al., 2011). In line with these studies, we found that freshly isolated cerebrovessels from r-mTBI animals (6 months post-injury) secreted significantly higher levels of Ang-1 compared to r-sham animals, while cerebrovascular Ang-2 secretion was unchanged between the r-mTBI and r-sham animals.

## Conclusions

These studies indicate tau elimination from the brain is diminished following r-mTBI, which may be the result of decreased caveolin-1-mediated tau transit across the BBB. Our prior work showed mural cell dysfunction and decreased cerebrovascular tau uptake coinciding with reduced caveolin-1 expression in the chronic phase following r-mTBI. The current studies suggest the changes in caveolin-1 post-injury may be due to alterations in mfsd2a expression in the BBB as a result of increased ang-1 secretion from dysfunctional pericytes in the aftermath of brain injury. Taken together, aberrant mural cell function following r-mTBI diminishes caveolae-mediated tau elimination across the BBB, which may describe the accumulation of tau deposits typically observed in the brain chronically following head trauma.

## **Declarations**

### **Ethics approval and consent to participate.**

All experiments using animals were performed under protocols approved by the Institutional Animal Care and Use Committee (IACUC) of the Roskamp Institute.

### **Consent for publication**

Not applicable.

### **Availability of data and materials**

The datasets during and/or analyzed during the current study available from the corresponding author on reasonable request.

### **Competing interests**

The authors declare they have no competing interests.

### **Funding**

This work was supported by the Department of Defense under award number W81XWH-16-1-0724-PRARP-CSRA. Opinions, interpretations, conclusions, and recommendations are those of the author and are not necessarily endorsed by the Department of Defense. This work was also supported by Merit Review award number I01BX003709 from the Department of Veterans Affairs (VA) Biomedical Laboratory Research and Development Program. The contents do not represent the views of the Department of Veterans Affairs or the United States Government. Dr. Bachmeier is a Research Scientist at the Bay Pines VA Healthcare System, Bay Pines, FL. Dr. Mouzon is a Research Scientist at the James A. Haley Veterans Hospital, Tampa, FL. Dr. Crawford is a Research Career Scientist at the James A. Haley Veterans Hospital, Tampa, FL. Finally, we would like to thank the Roskamp Institute for their generosity in helping to make this work possible.

### **Author Contributions**

All authors had full access to the data in the study and take responsibility for the integrity of the data and the accuracy of the data analysis. Conceptualization, M.E., A.P., M.M., F.C., J.O. and C.B.; Methodology, M.E. and C.B.; Investigation, M.E., A.P., A.G., J.O., and C.B.; Formal Analysis, M.E., A.P., and C.B.; Resources, M.M., F.C., and C.B.; Writing – Original Draft, M.E. and C.B.; Writing – Review and Editing, M.E., A.P., J.O., B.M., and C.B.; Visualization, M.E., A.P., and C.B.; Supervision, M.M. and F.C.; Funding Acquisition, C.B.

## Acknowledgements

Not applicable.

## Significance Statement

Traumatic brain injury (TBI) can lead to the accumulation of pathogenic tau proteins, but the mechanisms governing tau elimination from the brain are not entirely understood. Our studies indicated tau can be eliminated across the blood-brain barrier and that tau elimination from the brain is diminished post-injury. As the cerebrovasculature degenerates in the chronic phase following TBI, the pathways governing tau elimination at the BBB are downregulated, which may contribute to the accumulation of tau species in the brain post-injury. These studies further our understanding of tau elimination from the brain and the influence of TBI on these processes.

## References

- Andorfer, C. *et al.* (2003) "Hyperphosphorylation and aggregation of tau in mice expressing normal human tau isoforms," *Journal of Neurochemistry*, 86(3), pp. 582–590. doi: 10.1046/j.1471-4159.2003.01879.x.
- Andreone, B. J. *et al.* (2017) "Blood-Brain Barrier Permeability Is Regulated by Lipid Transport-Dependent Suppression of Caveolae-Mediated Transcytosis," *Neuron*, 94(3), pp. 581-594.e5. doi: 10.1016/j.neuron.2017.03.043.
- Bachmeier, C. *et al.* (2014) "Apolipoprotein E Isoform-Specific Effects on Lipoprotein Receptor Processing," *NeuroMolecular Medicine*, 16(4), pp. 686–696. doi: 10.1007/s12017-014-8318-6.
- Bachmeier, C., Mullan, M. and Paris, D. (2010) "Characterization and use of human brain microvascular endothelial cells to examine  $\beta$ -amyloid exchange in the blood-brain barrier," *Cytotechnology*, 62(6), pp. 519–529. doi: 10.1007/s10616-010-9313-x.
- Badaut, J. *et al.* (2015) "Caveolin expression changes in the neurovascular unit after juvenile traumatic brain injury: Signs of blood-brain barrier healing?," *Neuroscience*, 285, pp. 215–226. doi: 10.1016/j.neuroscience.2014.10.035.
- Banks, W. A. (2015) "The blood-brain barrier in neuroimmunology: Tales of separation and assimilation," *Brain, Behavior, and Immunity*, 44, pp. 1–8. doi: 10.1016/j.bbi.2014.08.007.

- Banks, W. A. *et al.* (2016) "Tau proteins cross the blood-brain barrier," *Journal of Alzheimer's Disease*, 55(1), pp. 411–419. doi: 10.3233/JAD-160542.
- Ben-Zvi, A. *et al.* (2014) "Mfsd2a is critical for the formation and function of the blood-brain barrier," *Nature*, 509(7501), pp. 507–511. doi: 10.1038/nature13324.
- Bonds, J. A. *et al.* (2019) "Depletion of Caveolin-1 in Type 2 Diabetes Model Induces Alzheimer's Disease Pathology Precursors," *The Journal of neuroscience: the official journal of the Society for Neuroscience*, 39(43), pp. 8576–8583. doi: 10.1523/JNEUROSCI.0730-19.2019.
- Brickler, T. R. *et al.* (2018) "Angiopoietin/tie2 axis regulates the age-at-injury cerebrovascular response to traumatic brain injury," *Journal of Neuroscience*, 38(45), pp. 9618–9634. doi: 10.1523/JNEUROSCI.0914-18.2018.
- Clavaguera, F. *et al.* (2009) "Transmission and spreading of tauopathy in transgenic mouse brain," *Nature Cell Biology*, 11(7), pp. 909–913. doi: 10.1038/ncb1901.
- David, D. C. *et al.* (2002) "Proteasomal degradation of tau protein," *Journal of Neurochemistry*, 83(1), pp. 176–185. doi: 10.1046/j.1471-4159.2002.01137.x.
- Deane, R. *et al.* (2009) "Endothelial protein C receptor-assisted transport of activated protein C across the mouse blood-brain barrier," *Journal of Cerebral Blood Flow and Metabolism*, 29(1), pp. 25–33. doi: 10.1038/jcbfm.2008.117.
- Dolan, P. J. and Johnson, G. V. W. (2010) "A caspase cleaved form of tau is preferentially degraded through the autophagy pathway," *Journal of Biological Chemistry*, 285(29), pp. 21978–21987. doi: 10.1074/jbc.M110.110940.
- Dore-Duffy, P. *et al.* (2007) "Differential expression of capillary VEGF isoforms following traumatic brain injury," *Neurological Research*, 29(4), pp. 395–403. doi: 10.1179/016164107X204729.
- Engelhardt, B. and Liebner, S. (2014) "Novel insights into the development and maintenance of the blood-brain barrier," *Cell and Tissue Research*. Springer Verlag, pp. 687–699. doi: 10.1007/s00441-014-1811-2.
- Eser Ocak, P., Ocak, U., Sherchan, P., Zhang, J. H., *et al.* (2020) "Insights into major facilitator superfamily domain-containing protein-2a (Mfsd2a) in physiology and pathophysiology. What do we know so far?," *Journal of Neuroscience Research*. John Wiley and Sons Inc., pp. 29–41. doi: 10.1002/jnr.24327.
- Eser Ocak, P., Ocak, U., Sherchan, P., Gamdzyk, M., *et al.* (2020) "Overexpression of Mfsd2a attenuates blood brain barrier dysfunction via Cav-1/Keap-1/Nrf-2/HO-1 pathway in a rat model of surgical brain injury," *Experimental Neurology*, 326. doi: 10.1016/j.expneurol.2020.113203.
- Evans, L. D. *et al.* (2018) "Extracellular Monomeric and Aggregated Tau Efficiently Enter Human Neurons through Overlapping but Distinct Pathways," *Cell Reports*, 22(13), pp. 3612–3624. doi:

10.1016/j.celrep.2018.03.021.

Felcht, M. *et al.* (2012) "Angiopoietin-2 differentially regulates angiogenesis through TIE2 and integrin signaling," *Journal of Clinical Investigation*, 122(6), pp. 1991–2005. doi: 10.1172/JCI58832.

Frost, B., Jacks, R. L. and Diamond, M. I. (2009) "Propagation of Tau misfolding from the outside to the inside of a cell," *Journal of Biological Chemistry*, 284(19), pp. 12845–12852. doi: 10.1074/jbc.M808759200.

Gaengel, K. *et al.* (2009) "Endothelial-mural cell signaling in vascular development and angiogenesis," *Arteriosclerosis, Thrombosis, and Vascular Biology*, pp. 630–638. doi: 10.1161/ATVBAHA.107.161521.

Gill, J. *et al.* (2017) "Acute plasma tau relates to prolonged return to play after concussion," *Neurology*, 88(6), pp. 595–602. doi: 10.1212/WNL.0000000000003587.

Gong, D. *et al.* (2011) "Dynamic changes of vascular endothelial growth factor and angiopoietin-1 in association with circulating endothelial progenitor cells after severe traumatic brain injury," *Journal of Trauma - Injury, Infection and Critical Care*, 70(6), pp. 1480–1484. doi: 10.1097/TA.0b013e31821ac9e1.

Gu, H. *et al.* (2016) "Angiopoietin-1 and angiopoietin-2 expression imbalance influence in early period after subarachnoid hemorrhage," *International Neurology Journal*, 20(4), pp. 288–295. doi: 10.5213/inj.1632692.346.

Hansen, T. M. *et al.* (2010) "Effects of angiopoietins-1 and -2 on the receptor tyrosine kinase Tie2 are differentially regulated at the endothelial cell surface," *Cellular Signalling*, 22(3), pp. 527–532. doi: 10.1016/j.cellsig.2009.11.007.

Head, B. P. *et al.* (2010) "Loss of caveolin-1 accelerates neurodegeneration and aging," *PLoS ONE*, 5(12), pp. 1–13. doi: 10.1371/journal.pone.0015697.

Iliff, J. J. *et al.* (2014) "Impairment of glymphatic pathway function promotes tau pathology after traumatic brain injury," *Journal of Neuroscience*, 34(49), pp. 16180–16193. doi: 10.1523/JNEUROSCI.3020-14.2014.

Jozic, I. *et al.* (2019) "Pharmacological and Genetic Inhibition of Caveolin-1 Promotes Epithelialization and Wound Closure," *Molecular Therapy*, 27(11), pp. 1992–2004. doi: 10.1016/j.ymthe.2019.07.016.

Kim, I. *et al.* (2000) "Angiopoietin-1 regulates endothelial cell survival through the phosphatidylinositol 3'-kinase/Akt signal transduction pathway," *Circulation Research*, 86(1), pp. 24–29. doi: 10.1161/01.RES.86.1.24.

Kurmann, L. *et al.* (2021) "Transcriptomic Analysis of Human Brain-Microvascular Barrier Function," *Cells*, 10, pp. 1–23. doi: 10.3390/cells10040963.

Laksitorini, M. D. *et al.* (2019) "Modulation of Wnt/ $\beta$ -catenin signaling promotes blood-brain barrier phenotype in cultured brain endothelial cells," *Scientific Reports*, 9(1), pp. 1–13. doi: 10.1038/s41598-019-56075-w.

Magnoni, S. *et al.* (2012) "Tau elevations in the brain extracellular space correlate with reduced amyloid- $\beta$  levels and predict adverse clinical outcomes after severe traumatic brain injury," *Brain*, 135(4), pp. 1268–1280. doi: 10.1093/brain/awr286.

Marklund, N. *et al.* (2009) "Monitoring of brain interstitial total tau and beta amyloid proteins by microdialysis in patients with traumatic brain injury: Clinical article," *Journal of Neurosurgery*, 110(6), pp. 1227–1237. doi: 10.3171/2008.9.JNS08584.

McKee, A. C. *et al.* (2009) "Chronic traumatic encephalopathy in athletes: Progressive tauopathy after repetitive head injury," *Journal of Neuropathology and Experimental Neurology*, pp. 709–735. doi: 10.1097/NEN.0b013e3181a9d503.

McKee, A. C. *et al.* (2016) "The first NINDS/NIBIB consensus meeting to define neuropathological criteria for the diagnosis of chronic traumatic encephalopathy," *Acta Neuropathologica*, 131(1), pp. 75–86. doi: 10.1007/s00401-015-1515-z.

Medina, M. and Avila, J. (2014) "The role of extracellular Tau in the spreading of neurofibrillary pathology," *Frontiers in Cellular Neuroscience*. Frontiers Research Foundation. doi: 10.3389/fncel.2014.00113.

Mirbaha, H. *et al.* (2017) "Inert and seed-competent tau monomers suggest structural origins of aggregation," *bioRxiv*, pp. 1–29. doi: 10.1101/163394.

Mouzon, B. *et al.* (2012) "Repetitive mild traumatic brain injury in a mouse model produces learning and memory deficits accompanied by histological changes," *Journal of Neurotrauma*, 29(18), pp. 2761–2773. doi: 10.1089/neu.2012.2498.

Mouzon, B. C. *et al.* (2014) "Chronic neuropathological and neurobehavioral changes in a repetitive mild traumatic brain injury model," *Annals of Neurology*, 75(2), pp. 241–254. doi: 10.1002/ana.24064.

Nag, S. *et al.* (2017) "Molecular Changes Associated with the Protective Effects of Angiopoietin-1 During Blood-Brain Barrier Breakdown Post-Injury," *Molecular Neurobiology*, 54(6), pp. 4232–4242. doi: 10.1007/s12035-016-9973-4.

Natarajan, R., Northrop, N. and Yamamoto, B. (2017) "Fluorescein isothiocyanate (FITC)-dextran extravasation as a measure of blood-brain barrier permeability," *Current Protocols in Neuroscience*, 2017, pp. 9.58.1-9.58.15. doi: 10.1002/cpns.25.

Nimmo, J. *et al.* (2020) "Peri-arterial pathways for clearance of  $\alpha$ -Synuclein and tau from the brain: Implications for the pathogenesis of dementias and for immunotherapy," *Alzheimer's and Dementia*:

*Diagnosis, Assessment and Disease Monitoring*, 12(1), pp. 1–10. doi: 10.1002/dad2.12070.

Nourhaghighi, N. *et al.* (2003) "Altered expression of angiopoietins during blood-brain barrier breakdown and angiogenesis," *Laboratory Investigation*, 83(8), pp. 1211–1222. doi: 10.1097/01.LAB.0000082383.40635.FE.

Ojo, J. *et al.* (2021) "Mural cell dysfunction leads to altered cerebrovascular tau uptake following repetitive head trauma," *Neurobiology of Disease*, 150(December 2020), p. 105237. doi: 10.1016/j.nbd.2020.105237.

Öst, M. *et al.* (2006) "Initial CSF total tau correlates with 1-year outcome in patients with traumatic brain injury," *Neurology*, 67(9), pp. 1600–1604. doi: 10.1212/01.wnl.0000242732.06714.0f.

Paris, D. *et al.* (2011) "Selective antihypertensive dihydropyridines lower A $\beta$  accumulation by targeting both the production and the clearance of A $\beta$  across the blood-brain barrier," *Molecular Medicine*, 17(3–4), pp. 149–162. doi: 10.2119/molmed.2010.00180.

Park, Y. S. *et al.* (2016) "Expression of angiopoietin-1 in hypoxic pericytes: Regulation by hypoxia-inducible factor-2 $\alpha$  and participation in endothelial cell migration and tube formation," *Biochemical and Biophysical Research Communications*, 469(2), pp. 263–269. doi: 10.1016/j.bbrc.2015.11.108.

Potje, S. R. *et al.* (2019) "Reduced caveolae density in arteries of SHR contributes to endothelial dysfunction and ROS production," *Scientific Reports*, 9(1). doi: 10.1038/s41598-019-43193-8.

Sabirzhanov, B. *et al.* (2018) "MicroRNA-711-Induced Downregulation of Angiopoietin-1 Mediates Neuronal Cell Death," *Journal of Neurotrauma*, 35(20), pp. 2462–2481. doi: 10.1089/neu.2017.5572.

Salehi, A., Zhang, J. H. and Obenaus, A. (2017) "Response of the cerebral vasculature following traumatic brain injury," *Journal of Cerebral Blood Flow and Metabolism*. SAGE Publications Ltd, pp. 2320–2339. doi: 10.1177/0271678X17701460.

Sato, C. *et al.* (2018) "Tau Kinetics in Neurons and the Human Central Nervous System," *Neuron*, 97(6), pp. 1284-1298.e7. doi: 10.1016/j.neuron.2018.02.015.

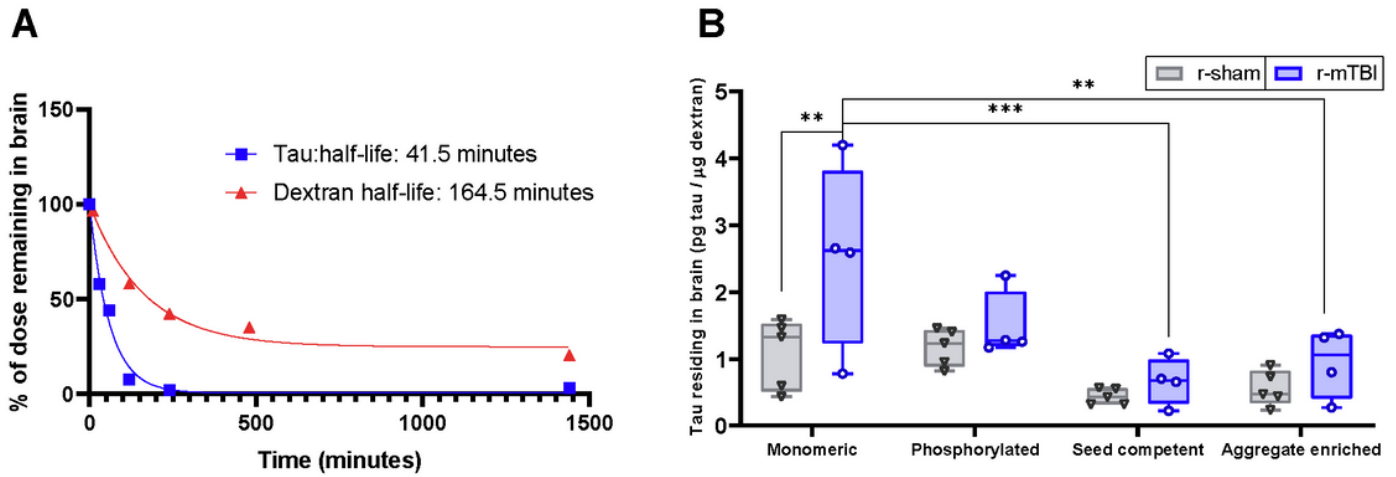
Sui, Y. T. *et al.* (2014) "Alpha synuclein is transported into and out of the brain by the blood-brain barrier," *Peptides*, 62, pp. 197–202. doi: 10.1016/j.peptides.2014.09.018.

Sun, Zhengyu. *et al.* (2021) "Reduction of Pericyte Coverage Leads to Blood- Brain Barrier Dysfunction Via Endothelial Transcytosis Following Chronic Cerebral Hypoperfusion," *Fluids and Barriers of the CNS*, 18(21), pp. 1–18. doi: 10.1186/s12987-021-00255-2.

Sundberg, C. *et al.* (2002) "Stable expression of angiopoietin-1 and other markers by cultured pericytes: Phenotypic similarities to a subpopulation of cells in maturing vessels during later stages of angiogenesis in vivo," *Laboratory Investigation*, 82(4), pp. 387–401. doi: 10.1038/labinvest.3780433.

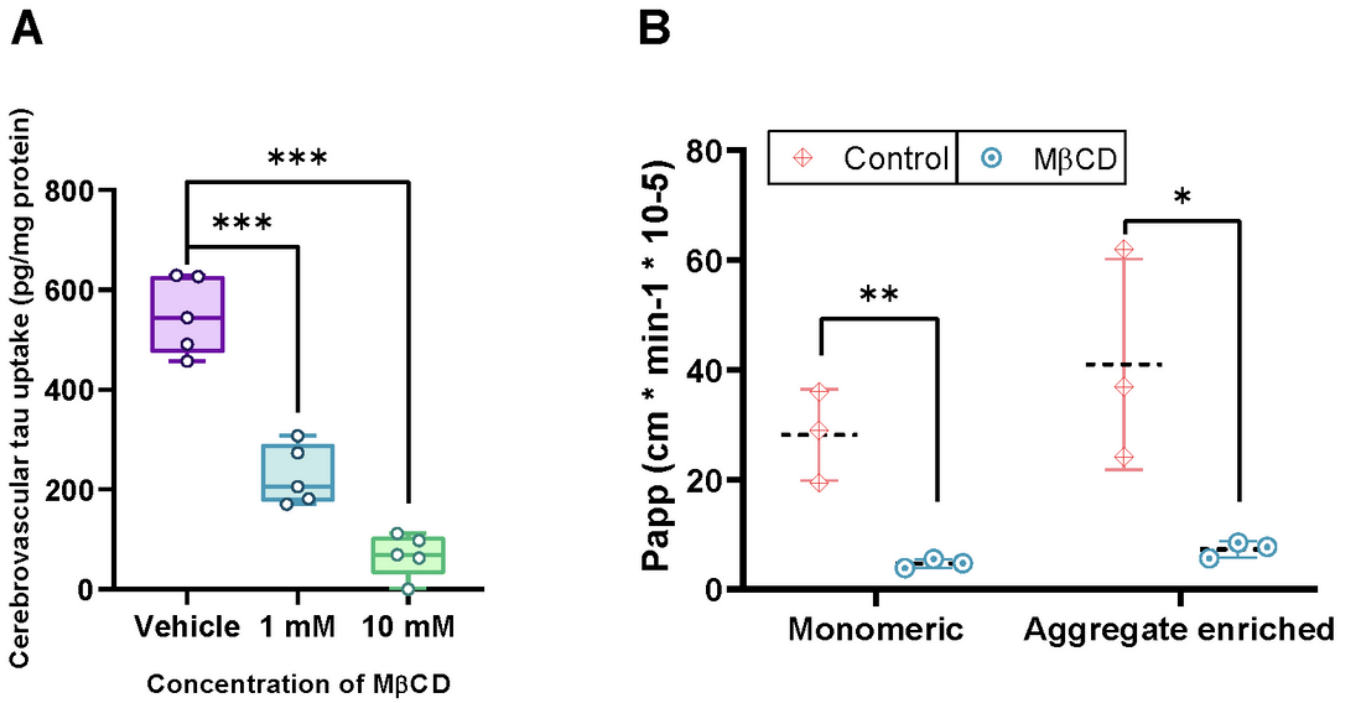
- Sweeney, M. D., Ayyadurai, S. and Zlokovic, B. v. (2016) "Pericytes of the neurovascular unit: Key functions and signaling pathways," *Nature Neuroscience*. Nature Publishing Group, pp. 771–783. doi: 10.1038/nn.4288.
- Tian, X. *et al.* (2020) "On the shuttling across the blood-brain barrier via tubules formation: Mechanism and cargo avidity bias," *bioRxiv*, (November), pp. 1–16. doi: 10.1101/2020.04.04.025866.
- Wang, J. *et al.* (2018) "Physiological clearance of tau in the periphery and its therapeutic potential for tauopathies," *Acta Neuropathologica*, 136(4), pp. 525–536. doi: 10.1007/s00401-018-1891-2.
- Wang, Z. *et al.* (2020) *Wnt signaling activates MFSD2A to suppress vascular endothelial transcytosis and maintain blood-retinal barrier*, *Sci. Adv.* Available at: <http://advances.sciencemag.org/>.
- Wu, J. W. *et al.* (2013) "Small misfolded tau species are internalized via bulk endocytosis and anterogradely and retrogradely transported in neurons," *Journal of Biological Chemistry*, 288(3), pp. 1856–1870. doi: 10.1074/jbc.M112.394528.
- Yamada, K. *et al.* (2011) "In vivo microdialysis reveals age-dependent decrease of brain interstitial fluid tau levels in P301S human tau transgenic mice," *Journal of Neuroscience*, 31(37), pp. 13110–13117. doi: 10.1523/JNEUROSCI.2569-11.2011.
- Yamada, K. *et al.* (2015) "Analysis of in vivo turnover of tau in a mouse model of tauopathy," *Molecular Neurodegeneration*, 10(1). doi: 10.1186/s13024-015-0052-5.
- Yanamandra, K. *et al.* (2017) "Anti-tau antibody administration increases plasma tau in transgenic mice and patients with tauopathy," *Science Translational Medicine*, 9(386). doi: 10.1126/scitranslmed.aal2029.
- Yang, A. C. *et al.* (2020) "Physiological blood–brain transport is impaired with age by a shift in transcytosis," *Nature*, 583(7816), pp. 425–430. doi: 10.1038/s41586-020-2453-z.
- Yang, Y. R. *et al.* (2017) "Mfsd2a (major facilitator superfamily domain containing 2a) attenuates intracerebral hemorrhage-induced blood-brain barrier disruption by inhibiting vesicular transcytosis," *Journal of the American Heart Association*, 6(7). doi: 10.1161/JAHA.117.005811.
- Zhang, J. *et al.* (2011) "Angiopoietin-1/Tie2 signal augments basal notch signal controlling vascular quiescence by inducing delta-like 4 expression through AKT-mediated activation of  $\beta$ -catenin," *Journal of Biological Chemistry*, 286(10), pp. 8055–8066. doi: 10.1074/jbc.M110.192641.
- Zhao, C. *et al.* (2020) "Mfsd2a Attenuates Blood-Brain Barrier Disruption After Sub-arachnoid Hemorrhage by Inhibiting Caveolae-Mediated Transcellular Transport in Rats," *Translational Stroke Research*, 11(5), pp. 1012–1027. doi: 10.1007/s12975-019-00775-y.

## Figures



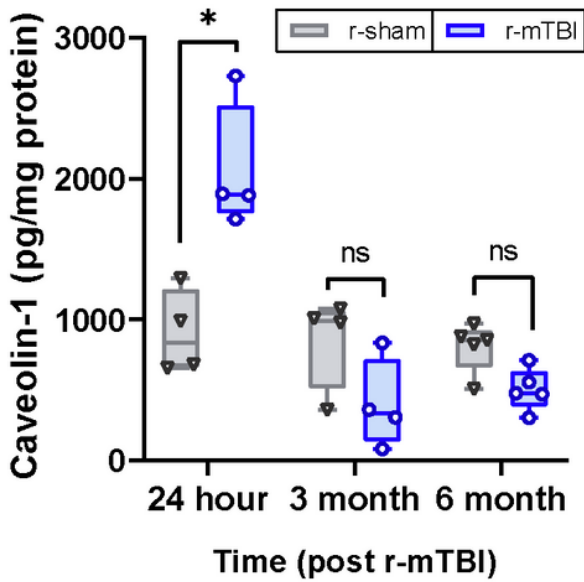
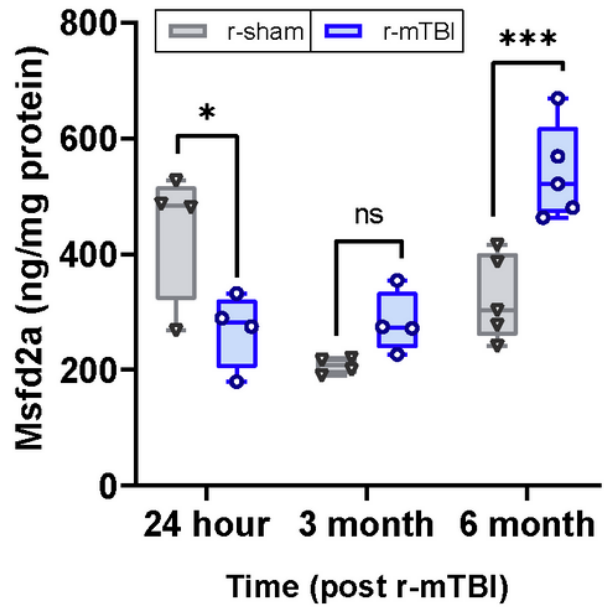
**Figure 1**

Effect of r-mTBI on the elimination of exogenous tau species from the brain. (A) The time course of tau elimination from the brain was established by examining bttau (n = 6) and 10 kDa LyD (n = 5) levels in the brain at various time points following intracortical injection into wild-type mice. Btau content was analyzed using an ELISA and LyD was analyzed via fluorescence. The half-life for both bttau and LyD were determined using nonlinear regression and a one phase decay fit. (B) Following intracortical injection in r-sham (n = 10) and r-mTBI mice (n = 8) (12 months post-injury), the amount of exogenous bttau species residing in the brain was determined at 2 hours post-injection. For each injection, bttau was co-injected with LyD. Btau content was analyzed using an ELISA while LyD was analyzed via fluorescence. Values represent mean + SD (n = 4-5) and are expressed as pg of tau per  $\mu$ g of LyD. \*\*P < 0.01, \*\*\*P < 0.001 as compared to r-sham as determined by a two-way ANOVA and Bonferroni post-hoc test.



**Figure 2**

Effect of MβCD on tau transcytosis across an in vitro model of the BBB. (A) Freshly isolated cerebrovessels from 9 month-old WT mice were pretreated with various concentrations of the caveolin inhibitor MβCD (0, 1 mM, 10 mM) for 30 minutes at 37 °C, before being exposed to recombinant human tau (5 ng/ml) for 1 hour at 37 °C. Lysates were analyzed for tau content using ELISA and normalized total protein using the BCA assay. Values represent mean + SD (n = 5) and are expressed as pg of tau per mg of total protein. \*\*\*P < 0.001 compared to vehicle as determined by one-way ANOVA and Bonferroni post-hoc test. (B) MβCD (10 mM) was exposed to the basolateral compartment of the in vitro BBB model for 30 minutes at 37 °C. Following the pretreatment with MβCD, biotin-labeled monomeric or aggregate enriched bttau was added alongside the known paracellular marker 10 kDa LyD to the basolateral compartment of the in vitro BBB model. Samples were collected from the apical compartment at 0, 30, and 60 minutes to determine the permeability of bttau and LyD across the BBB model. Values represent mean ± SD (n = 3) and are expressed as the apparent permeability coefficient (Papp). \*P < 0.05, \*\*P < 0.01 compared to each respective tau species with vehicle as determined by unpaired t-Test.

**A****B****Figure 3**

Effect of r-mTBI on caveolin-1 and Mfsd2a levels in freshly isolated cerebrovessels from r-mTBI mice (24 hour, 3 months, 6 months post-last injury). Lysates were analyzed for (A) cav-1 and (B) Mfsd2a by ELISA and normalized to total protein using the BCA assay. Values represent mean + SD (n =4-5) and are expressed as pg of cav-1 or ng Mfsd2a per mg total protein. \*P < 0.05, \*\*\*P < 0.001 compared to each respective r-sham as determined by two-way ANOVA and Bonferroni's multiple comparisons test.

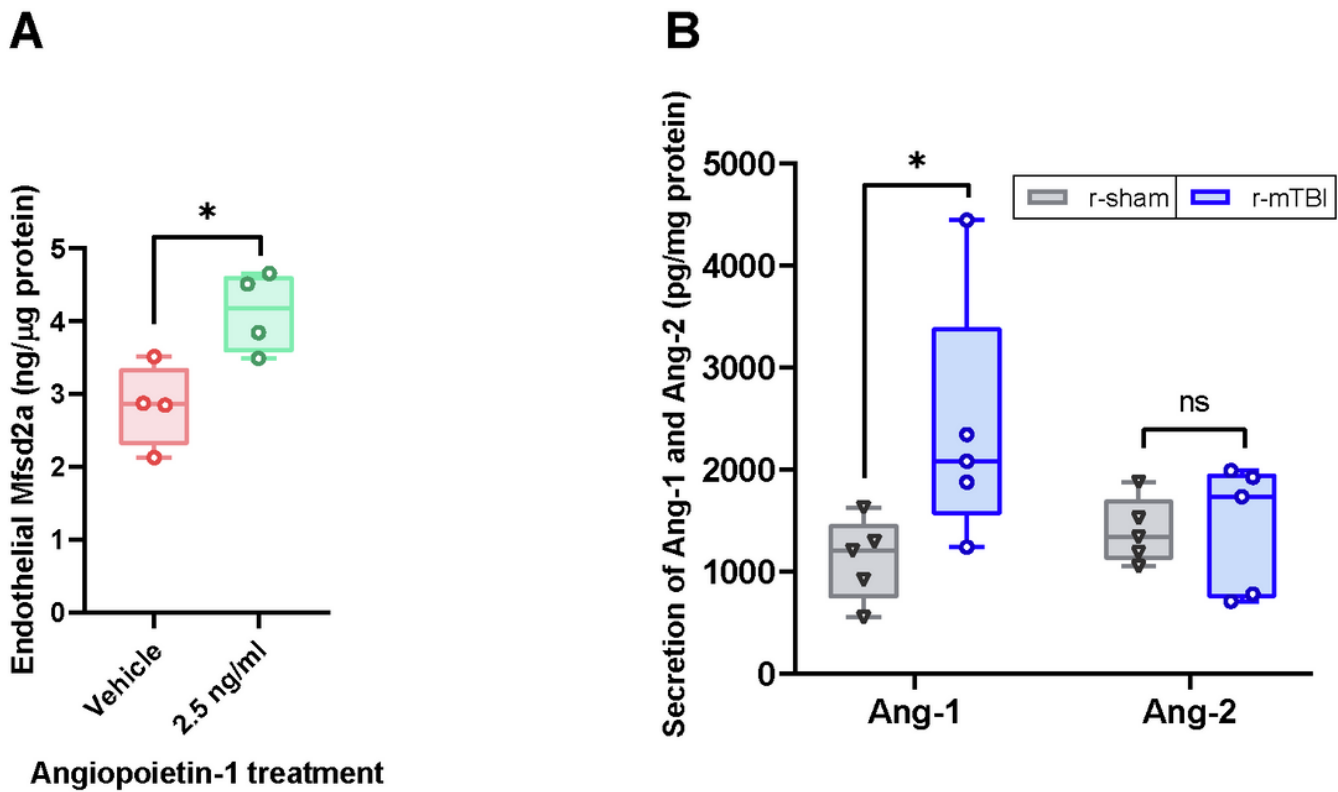


**Figure 4**

Influence of r-mTBI on cerebrovascular angiopoietin secretion. (A) Mfsd2a expression in HBMEC following treatment with Ang-1 (2.5 ng/ml) for 24 hours at 37 °C. Ang-1 expression was quantified by ELISA and normalized to total protein using the BCA assay. Values represent mean + SD (n = 4) and are expressed as ng Mfsd2a per μg of total protein. \*P < 0.05 compared to vehicle as determined by unpaired t-Test. (B) Secretion of Ang-1 and Ang-2 from fresh cerebrovessels isolated from r-sham and r-mTBI mice. Following 72 hours of incubation at 37 °C, the cerebrovascular extracellular media was probed for Ang-1 and Ang-2 using an ELISA and normalized to total protein using the BCA assay. Values represent mean + SD (n = 5) and are expressed as pg of Ang-1 or Ang-2 per mg total protein. \*P < 0.05 compared to each respective r-sham as determined by a Mann-Whitney U test.

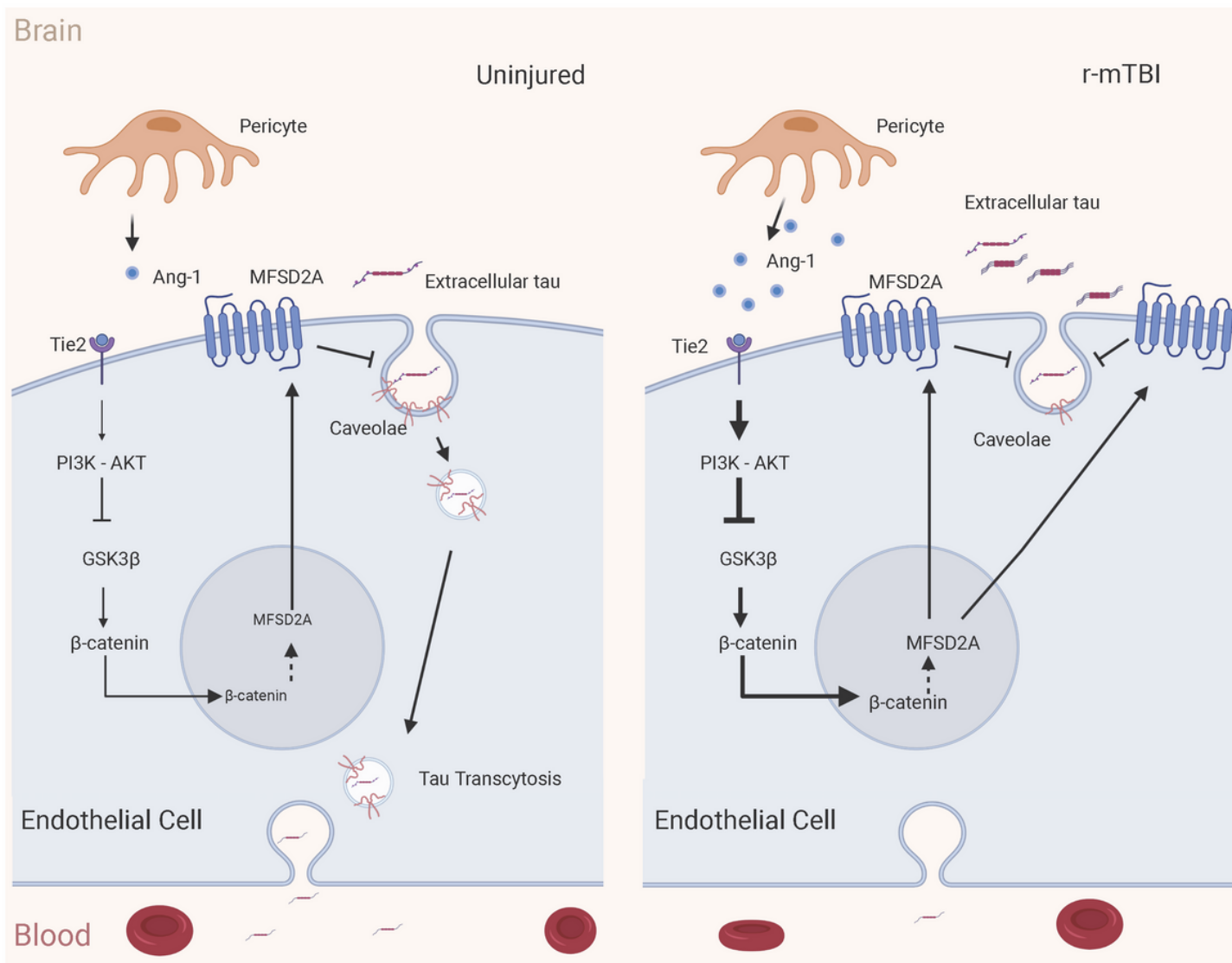


**Figure 5**

Proposed signaling cascade in brain endothelia following r-mTBI. In healthy aging, mural cells constitutively secrete Ang-1 which binds to endothelial Tie2 receptors and triggers the AKT-induced phosphorylation and inactivation of GSK3β. This allows translocation of β-catenin into the nucleus where it leads to the transcription of MfSD2a, which regulates the extent of caveolae-mediated transcytosis at the BBB. In the chronic phase following r-mTBI, Ang-1 secretion from reactive pericytes is elevated, which results in increased expression of MfSD2a and reduced caveolae-mediated transcytosis across the BBB. The diminished caveolae activity and tau elimination at the BBB could lead to an accumulation of tau in the brain, which is a key pathological signature in the chronic phase following trauma to the brain. Created with BioRender.com.